

Aberration of gravitational waveforms by peculiar velocity

Camille Bonvin^{1*}, Giulia Cusin^{1,2}, Cyril Pitrou², Simone Mastrogiovanni^{3,4},
Giuseppe Congedo⁵ and Jonathan Gair⁶

¹ *Université de Genève, Département de Physique Théorique and Centre for Astroparticle Physics, 24 quai Ernest-Ansermet, CH-1211 Genève 4, Switzerland*

² *Sorbonne Université, CNRS, UMR 7095, Institut d'Astrophysique de Paris, 75014 Paris, France*

³ *Artemis, Université Côte d'Azur, Observatoire de la Côte d'Azur, CNRS, F-06304 Nice, France*

⁴ *INFN, Sezione di Roma, I-00185 Roma, Italy*

⁵ *Institute for Astronomy, School of Physics and Astronomy, University of Edinburgh, Royal Observatory, Blackford Hill, Edinburgh, EH9 3HJ, United Kingdom,*

⁶ *Max-Planck-Institut für Gravitationsphysik, Albert-Einstein-Institut, Am Mühlenberg 1, 14476 Potsdam-Golm, Germany*

28 November 2022

ABSTRACT

One key prediction of General Relativity is that gravitational waves are emitted with a pure spin-2 polarisation. Any extra polarisation mode, spin-1 or spin-0, is consequently considered a smoking gun for deviations from General Relativity. In this paper, we show that the velocity of merging binaries with respect to the observer gives rise to spin-1 polarisation in the observer frame even in the context of General Relativity. These are pure projection effects, proportional to the plus and cross polarisations in the source frame, hence they do not correspond to new degrees of freedom. We demonstrate that the spin-1 modes can always be rewritten as pure spin-2 modes coming from an aberrated direction. Since gravitational waves are not isotropically emitted around binary systems, this aberration modifies the apparent orientation of the binary system with respect to the observer: the system appears slightly rotated due to the source velocity. Fortunately, this bias does not propagate to other parameters of the system (and therefore does not spoil tests of General Relativity), since the impact of the velocity can be fully reabsorbed into new orientation angles.

Key words: gravitational waves, compact binaries, kinematic aberration

1 INTRODUCTION

Binary systems of compact objects, like neutron stars or black holes, are predicted by General Relativity to emit gravitational waves (GW) with spin-2 polarisations. These spin-2 modes have been observed for the first time by the interferometer LIGO and Virgo in 2015 (Abbott et al. 2016) and from subsequent GW events (Abbott et al. 2019a, 2021a; The LIGO Scientific Collaboration et al. 2021a,c). From a theoretical point of view it is of crucial importance to model the expected signal as precisely as possible, in order to use these GW events to probe, on one hand, the physics of binary systems (Chen 2021), and, on the other hand, the validity of General Relativity (Abbott et al. 2019b, 2021b; The LIGO Scientific Collaboration et al. 2021d). A lot of effort has been devoted to calculate GW waveforms accounting for the relative velocity of the two objects in the binary, up to high order in the post-Newtonian expansion, see e.g. Blanchet (2014); Isoyama et al. (2021); Sturani (2021);

Zhao et al. (2021) for a more recent review. However, these frameworks usually neglect the fact that the centre of mass of the binary is itself moving with respect to the observer, due to the gravitational interaction with the host galaxy, host cluster, and the large-scale structure of the Universe.

Recently several studies have started exploring the effect of the binary peculiar velocity on the waveform of a GW signal. In particular, it has been found that the variation of the velocity during the time of observation modifies the waveform in a non-negligible way, an effect that is relevant for an interferometer like LISA, that will follow GW signals during months and even years, see e.g. Bonvin et al. (2017); Tamanini et al. (2020); Toubiana et al. (2021); Sberna et al. (2022). Other authors have addressed the impact of the binary peculiar motion for cosmological studies (Mukherjee et al. 2021). However, all these works focus on kinematic distortions of the amplitude and phase of the wave, assuming that the two emitted polarisations are affected in the same way by kinematic effects, i.e. effectively neglecting the spin-2 (tensorial) nature of the wave and treating the two wave polarisations as scalar waves. This is of course an approxi-

* camille.bonvin@unige.ch

mation, as we know that a GW is in fact a spin-2 quantity, which consequently transforms as a rank-2 tensor under a Lorentz boost.

In this paper, we study the effect of the binary peculiar velocity on the observed signal, accounting for the full polarisation structure of the GW. We show that the component of the binary velocity orthogonal to the line of sight (hereafter *transverse* velocity) changes the antenna pattern of an interferometer, generating spin-1 modes. Moreover, for a network of detectors, the transverse velocity changes also the time delay between interferometers (or similarly the phase shift). In Fig. 1 we plot the effect of various wave polarisations on a ring of test particles. Spin-1 polarisations give a vectorial deformation of the ring along the direction of propagation of the wave.

We then show that since the spin-1 modes have the same time dependence as the spin-2 modes, they can always be rewritten as spin-2 modes coming from an aberrated direction, and with a mixing of the two polarisations. Moreover, we show that the time delay between different interferometers can be rewritten in terms of the same aberrated direction. This means that only the aberrated direction and the aberrated polarisations can be measured. Importantly, the aberrated direction which allows us to re-absorb spin-1 modes into spin-2 modes is the same as the aberrated direction inferred from the propagation of electromagnetic signals emitted by moving sources. As a consequence, detecting a luminous counterpart would not help in reconstructing the spin-1 modes, nor measuring the binary transverse velocity.

Since GW emission is not isotropic, aberration and the mixing of polarisations have a direct impact on the amplitude of the detected signal. When reconstructing the parameters of the binary system from the detected signal, we find that the angles describing the orientation of the binary system are biased by the transverse peculiar velocity: the system appears rotated with respect to the observer. Fortunately, this effect has no impact on the other parameters of the system, like the luminosity distance or the chirp mass,¹ since the transverse velocity can be fully reabsorbed into an aberrated direction and mixed polarisations. As a consequence transverse velocities do not invalidate reconstruction of cosmological and astrophysical parameters with GWs.

The rest of the paper is structured as follows: after an overview of general concepts in Section 2, we present a detailed derivation of velocity-induced effects on the polarisation structure of the wave in Section 3. In Section 4 we show how spin-1 components can be re-written as spin-2 components coming from an aberrated direction and in Section 5 we demonstrate that the time-delay is proportional to this same aberrated direction. In Section 6 we discuss the observational impact of aberration and we conclude in Section 7. Technical derivations are presented in a series of appendices.

Notation: we work with units where the speed of light is set to one, $c = 1$. With v_1 and v_2 we denote projections of the source peculiar velocity orthogonal to the line of sight, and with v_3 the component along the line of sight. We de-

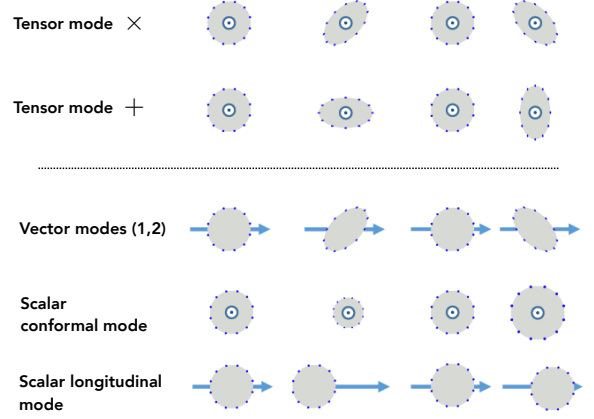


Figure 1. Effect of different wave polarisations on a sphere of test-particles.

note with a tilde quantities in the source frame, and without tilde quantities in the observer frame (that we will also refer to as *aberrated frame*). Moreover, since typically we expect peculiar velocities to be non-relativistic, in our computation we keep only linear order terms in v/c . This leads to simpler formulas whose physical interpretation is more transparent.

2 GENERAL CONCEPTS

We start by reviewing the standard result of detector arm-length variation induced by an incoming GW emitted by a source which is at rest with respect to the interferometer. This will serve as a basis for Section 3 where we show how this derivation is modified if the source is moving. We consider two test particles in free fall, i.e. moving on nearby geodesics. The vector connecting these two geodesics, ξ^μ , obeys the geodesic deviation equation

$$\frac{D^2 \xi^\mu}{D\tau^2} = -\mathcal{R}^\mu_{\nu\rho\sigma} \xi^\rho u^\nu u^\sigma, \quad (1)$$

where τ is the proper time of the particles and u^μ is their four-velocity. In the frame of the particles, which we call “observer frame”, we have by construction $u^\mu = (-1, 0, 0, 0)$, and the geodesic deviation equation becomes

$$\frac{d^2 \xi^i}{dt^2} = -S_{ij} \xi^j. \quad (2)$$

Here t is the coordinate time, which is related to the proper time by $u^0 = -dt/d\tau = -1$, and S is the *driving force matrix*, defined as

$$S_{ij} \equiv \mathcal{R}_{0i0j}, \quad (3)$$

where i, j span the spatial coordinates x, y, z .

The passage of a GW affects the Riemann tensor and consequently the driving force matrix. We perturb the Minkowski metric as $g_{\mu\nu} = \eta_{\mu\nu} + h_{\mu\nu}$. At linear order in the perturbation $h_{\mu\nu}$, the Riemann tensor is given by $\mathcal{R}^{\mu\nu}_{\rho\sigma} = -2\partial^{[\mu}\partial_{[\rho}h_{\sigma]}^{\nu]}$ which is manifestly invariant under an infinitesimal gauge transformation $g_{\mu\nu} \rightarrow g_{\mu\nu} - \partial_\mu \xi_\nu - \partial_\nu \xi_\mu$.

¹ These quantities are of course affected by the longitudinal component of the velocity through Doppler effects, but there are not affected by the transverse velocity which aberrates the signal and mixes the polarisations.

From (3) the linear order driving force matrix reads

$$S_{ij} = \frac{1}{2} (-\partial_i \partial_j h_{00} + \partial_0 \partial_j h_{0i} - \partial_0 \partial_0 h_{ij} + \partial_i \partial_0 h_{0j}). \quad (4)$$

Usually, one assumes that the source emitting a GW is at rest with respect to the observer. The metric in the wave zone can then be written in the transverse traceless (TT) gauge and the driving force matrix reduces to

$$S_{ij} = -\frac{1}{2} \ddot{h}_{ij}^{\text{TT}}, \quad (5)$$

leading to

$$\frac{d^2 \xi^i}{dt^2} = \frac{1}{2} \ddot{h}_{ij}^{\text{TT}} \xi^j, \quad (6)$$

with dots denoting differentiation with respect to t . For example, for a given Fourier mode with energy E in the observer frame, propagating along the z -direction, the driving force matrix reads

$$S_{ij} = \frac{E^2}{2} \begin{pmatrix} h_+ & h_\times & 0 \\ h_\times & -h_+ & 0 \\ 0 & 0 & 0 \end{pmatrix}, \quad (7)$$

where h_+ and h_\times denote the two polarisations of the GW.

The signal observed in an interferometer (called the strain and denoted by h) is directly proportional to the difference in length between its two arms. This is obtained by integrating twice Eq. (6) to find the change in length induced by the passing of the GW. For an interferometer with arms pointing in direction $\hat{\mathbf{l}}$ and $\hat{\mathbf{m}}$, in the long-wavelength regime,² one finds that the strain is given by

$$h = \frac{1}{2} (\hat{l}_i \hat{l}_j - \hat{m}_i \hat{m}_j) P_{ij}, \quad (8)$$

where

$$P_{ij} \equiv \frac{2}{E^2} S_{ij}. \quad (9)$$

The E^2 factor comes from the double integration over time when solving for ξ^i . We see that the dimensionless driving force matrix, P_{ij} , is the quantity that directly drives the amplitude of the detected GW signal. Note that for a monochromatic wave, the dimensionless driving force matrix is directly given by the metric in TT gauge: $P_{ij} = h_{ij}^{\text{TT}}$.

3 MOVING SOURCES

Let us now generalise these results to the case in which the source has a non-vanishing peculiar velocity with respect to the observer frame. In this case, we need to distinguish between quantities calculated in the observer frame, and quantities calculated in a frame comoving with the source (hereafter ‘‘source frame’’). Quantities in the source frame are denoted with a tilde. We denote by \mathbf{v} the velocity of the source with respect to the observer.

² For simplicity we assume that the long-wavelength approximation is valid, i.e. we ignore the effect of finite travel time of the photon. We note that this will not be acceptable for LISA and therefore one would need to properly account for the time delays in the response function. It is worth noting that an extra complication would be the much longer observation time at the mHz frequencies where the impact of the source’s velocity and acceleration would be even more important.

3.1 The dimensionless driving force matrix

We start by calculating the dimensionless driving force matrix. In the source frame, we write the metric in the TT gauge, i.e. we have $\tilde{h}_{00} = \tilde{h}_{0i} = 0$. The metric in the observer frame is related to the one in the source frame by a boost transformation Λ with velocity $-\mathbf{v}$:

$$h_{\mu\nu} = \Lambda_\mu^\alpha \Lambda_\nu^\beta \tilde{h}_{\alpha\beta}. \quad (10)$$

Keeping only terms that are linear in the velocity, we obtain (see Appendix A for details)

$$h_{00} = 0, \quad (11a)$$

$$h_{0i} = v_m \tilde{h}_{mi}, \quad (11b)$$

$$h_{ij} = \tilde{h}_{ij}. \quad (11c)$$

The geodesic deviation equation in the observer frame is still given by Eq. (2), but the driving force matrix (5) has now a different form, due to the velocity of the source. Inserting Eqs. (11) into Eq. (4) we obtain

$$S_{ij} = \frac{1}{2} \left(-\partial_0^2 \tilde{h}_{ij} + v_m \partial_i \partial_0 \tilde{h}_{mj} + v_m \partial_j \partial_0 \tilde{h}_{mi} \right), \quad (12)$$

where ∂_μ denotes a derivative with respect to the spatial coordinate x^μ . Let us assume that \tilde{h} is a plane wave in the source frame. For a monochromatic wave we have:

$$\tilde{h}_{ij} = \mathcal{A}_{ij}(\tilde{\mathbf{k}}) \exp(i\tilde{k}_\mu \tilde{x}^\mu) + \mathcal{A}_{ij}^*(\tilde{\mathbf{k}}) \exp(-i\tilde{k}_\mu \tilde{x}^\mu), \quad (13)$$

where $\tilde{k}^\mu = (-\tilde{E}, \tilde{k}^i)$ and $\tilde{x}^\mu = (-\tilde{\tau}, \tilde{x}^i)$. Since $\tilde{k}_\mu \tilde{x}^\mu = k_\mu x^\mu$, the partial derivatives are handled using that $\partial_\mu \partial_\nu$ brings a factor $-k_\mu k_\nu$. With $E \equiv k_0$ the energy in the observer frame, we get

$$\partial_0^2 \tilde{h}_{ij} = -E^2 \tilde{h}_{ij}, \quad (14a)$$

$$v_m \partial_0 \partial_i \tilde{h}_{mj} = -v_m k_i E \tilde{h}_{ij}, \quad (14b)$$

leading to

$$S_{ij} = \frac{1}{2} \left(E^2 \tilde{h}_{ij} - E v_m k_i \tilde{h}_{mj} - E v_m k_j \tilde{h}_{mi} \right). \quad (15)$$

The geodesic deviation equation in the observer frame is therefore directly affected by the peculiar velocity of the source. Note that in Eq. (15), E is shifted with respect to the energy in the source frame, \tilde{E} , by the velocity along the direction of propagation

$$E = \tilde{E}(1 + \mathbf{v} \cdot \hat{\mathbf{n}}), \quad (16)$$

where $\hat{\mathbf{n}}$ is a unit vector along the direction of propagation: $\hat{\mathbf{n}} \equiv \tilde{\mathbf{k}}/\tilde{k}$.

As before, the geodesic deviation equation must be solved to find the length difference between the two arms of an interferometer. Since $\tilde{h}_{\mu\nu}$ in Eq. (15) depends on the proper time of the source, $\tilde{\tau}$, we first rewrite Eq. (2) in terms of $\tilde{\tau}$ using that $dt = d\tau$ and that $d\tau = \tilde{E}/E d\tilde{\tau}$ (see Appendix C for a derivation of this equality). We obtain

$$\frac{d^2 \xi^i}{d\tilde{\tau}^2} = - \left(\frac{\tilde{E}}{E} \right)^2 S_{ij} \xi^j. \quad (17)$$

Using Eqs. (15) and (13), and integrating twice over proper time, we find that the dimensionless driving force matrix is given by

$$P_{ij} = \frac{2}{\tilde{E}^2} \left(\frac{\tilde{E}}{E} \right)^2 S_{ij} = \frac{2}{E^2} S_{ij}. \quad (18)$$

We see that the $1/\tilde{E}^2$ factor coming from the integration of $\tilde{h}_{\mu\nu}$ in Eq. (13) over proper time $\tilde{\tau}$ cancels the \tilde{E}^2 factor in Eq. (17). Note that the same result can be found by rewriting $\tilde{h}_{\mu\nu}$ in terms of quantities in the observer frame, using that $\tilde{k}_\mu \tilde{x}^\mu = k_\mu x^\mu$, and then integrating Eq. (2) directly over the proper time of the observer.

As an example, let us compute P_{ij} for a wave propagating along the z -direction (in the source frame), i.e. $\tilde{\mathbf{n}} = (0, 0, 1)$. Using that at zeroth order in the velocity $k_i = E n_i = E \tilde{n}_i$, leading to $E v_m k_i = E^2 v_m \tilde{n}_i$, and inserting Eq. (15) into (18) we obtain

$$P_{ij} = \begin{pmatrix} \tilde{h}_+ & \tilde{h}_\times & -v_x \tilde{h}_+ - v_y \tilde{h}_\times \\ \tilde{h}_\times & -\tilde{h}_+ & -v_x \tilde{h}_\times + v_y \tilde{h}_+ \\ -v_x \tilde{h}_+ - v_y \tilde{h}_\times & -v_x \tilde{h}_\times + v_y \tilde{h}_+ & 0 \end{pmatrix} \quad (19)$$

where \tilde{h}_+ and \tilde{h}_\times are the plus and cross polarisations in the source frame. Comparing Eq. (19) with Eq. (7), we see that the relative motion of the source with respect to the observer generates contributions to the dimensionless driving force matrix that are not transverse to the GW direction $\tilde{\mathbf{n}}$. P_{ij} in Eq. (19) has indeed non-zero contributions in direction zx and zy . In the next section we determine the observable impact of these non-transverse contributions.

In general, for a wave propagating in arbitrary direction, we define a set of orthonormal vectors, adapted to the incoming direction of the wave in the source frame

$$\tilde{\mathbf{n}} = (\sin \tilde{\theta} \cos \tilde{\phi}, \sin \tilde{\theta} \sin \tilde{\phi}, \cos \tilde{\theta}), \quad (20a)$$

$$\tilde{\mathbf{e}}_1(\tilde{\mathbf{n}}) = (\sin \tilde{\phi}, -\cos \tilde{\phi}, 0), \quad (20b)$$

$$\tilde{\mathbf{e}}_2(\tilde{\mathbf{n}}) = (\cos \tilde{\theta} \cos \tilde{\phi}, \cos \tilde{\theta} \sin \tilde{\phi}, -\sin \tilde{\theta}). \quad (20c)$$

With respect to these vectors, the metric in the TT gauge can be decomposed as

$$\tilde{h}_{ij}^{\text{TT}} = \tilde{h}_+ (\tilde{e}_{1i} \tilde{e}_{1j} - \tilde{e}_{2i} \tilde{e}_{2j}) + \tilde{h}_\times (\tilde{e}_{1i} \tilde{e}_{2j} + \tilde{e}_{2i} \tilde{e}_{1j}), \quad (21)$$

where it is implied that $\tilde{h}_{+, \times} = \tilde{h}_{+, \times}(\tilde{\mathbf{n}})$. Inserting this into Eqs. (15) and (18), and using as before that at linear order in the velocity $E v_m k_i = E^2 v_m \tilde{n}_i$, we obtain

$$P_{ij} = h_+ (\tilde{e}_{1i} \tilde{e}_{1j} - \tilde{e}_{2i} \tilde{e}_{2j}) + h_\times (\tilde{e}_{1i} \tilde{e}_{2j} + \tilde{e}_{2i} \tilde{e}_{1j}) + h_1 (\tilde{n}_i \tilde{e}_{1j} + \tilde{e}_{1i} \tilde{n}_j) + h_2 (\tilde{n}_i \tilde{e}_{2j} + \tilde{e}_{2i} \tilde{n}_j), \quad (22)$$

where

$$h_+ = \tilde{h}_+, \quad (23)$$

$$h_\times = \tilde{h}_\times,$$

$$h_1 = -v_1 \tilde{h}_+ - v_2 \tilde{h}_\times,$$

$$h_2 = -v_1 \tilde{h}_\times + v_2 \tilde{h}_+,$$

and we have defined the velocity component along the orthonormal set

$$v_1 \equiv \mathbf{v} \cdot \tilde{\mathbf{e}}_1, \quad v_2 \equiv \mathbf{v} \cdot \tilde{\mathbf{e}}_2, \quad v_3 \equiv \mathbf{v} \cdot \tilde{\mathbf{n}}. \quad (24)$$

As before, we see that the source velocity generates contributions to P_{ij} that are longitudinal: h_1 and h_2 are indeed along the direction of propagation $\tilde{\mathbf{n}}$.

Before moving to the calculation of the strain, let us comment on the relation between the dimensionless driving force matrix and the metric in the TT gauge. In the case of non-moving sources we saw that the dimensionless driving force matrix is equal to the metric in the TT gauge. For a

moving source we note that the symmetry between source and observer reference frames is broken. Hence fixing the TT gauge in one frame is no longer preserved under transformation on to the other frame. The dimensionless driving force matrix P_{ij} is therefore no longer equal to the metric in TT gauge *in the source frame*. However, we can apply another gauge transformation to the metric $h_{\mu\nu}$, to bring it in the TT gauge in the observer frame. In that case, we show in Appendix B that the resulting metric (B6) becomes equal to the dimensionless driving form matrix (19).

3.2 The strain

We now project the dimensionless driving force matrix P_{ij} onto the arms of an interferometer $\hat{\mathbf{l}}$ and $\hat{\mathbf{m}}$ to obtain the strain

$$h = \frac{1}{2} (\hat{l}_i \hat{l}_j - \hat{m}_i \hat{m}_j) P_{ij} \quad (25)$$

$$= F_+(\tilde{\mathbf{n}}) h_+ + F_\times(\tilde{\mathbf{n}}) h_\times + F_1(\tilde{\mathbf{n}}) h_1 + F_2(\tilde{\mathbf{n}}) h_2,$$

where the antenna patterns are given by

$$F_+(\tilde{\mathbf{n}}) = \frac{1}{2} (\hat{l}_i \hat{l}_j - \hat{m}_i \hat{m}_j) (\tilde{e}_{1i} \tilde{e}_{1j} - \tilde{e}_{2i} \tilde{e}_{2j}),$$

$$F_\times(\tilde{\mathbf{n}}) = \frac{1}{2} (\hat{l}_i \hat{l}_j - \hat{m}_i \hat{m}_j) (\tilde{e}_{1i} \tilde{e}_{2j} + \tilde{e}_{2i} \tilde{e}_{1j}),$$

$$F_1(\tilde{\mathbf{n}}) = \frac{1}{2} (\hat{l}_i \hat{l}_j - \hat{m}_i \hat{m}_j) (\tilde{n}_i \tilde{e}_{1j} + \tilde{e}_{1i} \tilde{n}_j),$$

$$F_2(\tilde{\mathbf{n}}) = \frac{1}{2} (\hat{l}_i \hat{l}_j - \hat{m}_i \hat{m}_j) (\tilde{n}_i \tilde{e}_{2j} + \tilde{e}_{2i} \tilde{n}_j). \quad (26)$$

As an example let us consider the strain response of an interferometer with arms pointing in the x and y directions: $\hat{\mathbf{l}} = (1, 0, 0)$ and $\hat{\mathbf{m}} = (0, 1, 0)$. We obtain

$$h = \frac{1}{2} (\hat{l}_i \hat{l}_j - \hat{m}_i \hat{m}_j) P_{ij} = -\frac{\tilde{h}_+}{2} (\cos^2 \tilde{\theta} + 1) \cos 2\tilde{\phi} + \tilde{h}_\times \cos \tilde{\theta} \sin 2\tilde{\phi} - (v_1 \tilde{h}_+ + v_2 \tilde{h}_\times) \sin \tilde{\theta} \sin 2\tilde{\phi} - (v_1 \tilde{h}_\times - v_2 \tilde{h}_+) \sin \tilde{\theta} \cos \tilde{\theta} \cos 2\tilde{\phi}. \quad (27)$$

From Eq. (27) we see that the transverse velocity of the source, namely the components v_1 and v_2 , generates contributions to the signal *which are not* proportional to the spin-2 antenna patterns

$$F_+(\tilde{\mathbf{n}}) = -\frac{1}{2} (\cos^2 \tilde{\theta} + 1) \cos 2\tilde{\phi}, \quad (28a)$$

$$F_\times(\tilde{\mathbf{n}}) = \cos \tilde{\theta} \sin 2\tilde{\phi}. \quad (28b)$$

These new contributions are proportional instead to spin-1 antenna patterns F_1 and F_2 .

In Eqs. (26) and (27) we have identified spin-2 modes as the contributions that are transverse to the direction of propagation of the GW, $\tilde{\mathbf{n}}$, in the source frame. This definition is somewhat arbitrary, since we do not observe $\tilde{\mathbf{n}}$ directly: we reconstruct it from the antenna patterns $F_+(\tilde{\mathbf{n}})$ and $F_\times(\tilde{\mathbf{n}})$. We can therefore wonder if there exists a direction \mathbf{n} such that the strain would contain only spin-2 polarisations *with respect to that direction*. In the next section we show that this is indeed the case, and that this new direction \mathbf{n} is nothing else than the aberrated direction obtained by applying the boost transformation on \tilde{k}^μ (and extracting the spatial part of the resulting vector).

4 ABERRATED REFERENCE FRAME

As for electromagnetic signals, we can define an aberrated momentum k^μ by applying the boost Λ^μ_ν on \tilde{k}^μ . The spatial part of k^μ is given by

$$k^i = \Lambda^i_\mu \tilde{k}^\mu = \tilde{E} \left(\tilde{n}^i + v^i \right), \quad (29)$$

leading to

$$\mathbf{n} \equiv \frac{\mathbf{k}}{|\mathbf{k}|} = \tilde{\mathbf{n}} + \mathbf{v} - v_3 \tilde{\mathbf{n}} = \tilde{\mathbf{n}} + \mathbf{v}_\perp, \quad (30)$$

where the transverse velocity \mathbf{v}_\perp is defined as

$$\mathbf{v}_\perp = \mathbf{v} - v_3 \tilde{\mathbf{n}}. \quad (31)$$

Note that this velocity is transverse to both \mathbf{n} and $\tilde{\mathbf{n}}$ since we neglect contributions quadratic in the velocity.

Let us start by calculating the strain for a detector with arms along xy , given by Eq. (27). From Eq. (30) we find that the aberrated angles are related to angles at the source by

$$\theta = \tilde{\theta} + \delta\theta = \tilde{\theta} + v_2, \quad (32a)$$

$$\phi = \tilde{\phi} + \delta\phi = \tilde{\phi} - \frac{v_1}{\sin\theta}. \quad (32b)$$

The apparent divergence at $\theta = 0$ is an artefact of the coordinate singularity there. The right ascension ϕ is indeed ambiguous at $\theta = 0$. Inserting this into Eq. (27) we obtain for the strain

$$h = \frac{1}{2} (\hat{l}_i \hat{l}_j - \hat{m}_i \hat{m}_j) P_{ij} = \tilde{h}_+ \left[F_+(\mathbf{n}) + 2v_1 \frac{\cos\theta}{\sin\theta} F_\times(\mathbf{n}) \right] + \tilde{h}_\times \left[F_\times(\mathbf{n}) - 2v_1 \frac{\cos\theta}{\sin\theta} F_+(\mathbf{n}) \right]. \quad (33)$$

We see that the source velocity induces a mixing between the two polarisations, proportional to F_+ and F_\times . Defining the polarisation angle

$$\delta\psi = -v_1 \frac{\cos\theta}{\sin\theta}, \quad (34)$$

we can rewrite Eq. (33) as

$$\begin{aligned} h &= \frac{1}{2} (\hat{l}_i \hat{l}_j - \hat{m}_i \hat{m}_j) P_{ij} \\ &= \tilde{h}_+ \left[F_+(\mathbf{n}) \cos(2\delta\psi) - F_\times(\mathbf{n}) \sin(2\delta\psi) \right] \\ &\quad + \tilde{h}_\times \left[F_\times(\mathbf{n}) \cos(2\delta\psi) + F_+(\mathbf{n}) \sin(2\delta\psi) \right] \\ &= \hat{h}_+(\mathbf{n}) F_+(\mathbf{n}) + \hat{h}_\times(\mathbf{n}) F_\times(\mathbf{n}), \end{aligned} \quad (35)$$

where we have defined

$$\hat{h}_+(\mathbf{n}) \equiv \tilde{h}_+(\tilde{\mathbf{n}}) \cos(2\delta\psi) + \tilde{h}_\times(\tilde{\mathbf{n}}) \sin(2\delta\psi), \quad (36a)$$

$$\hat{h}_\times(\mathbf{n}) \equiv \tilde{h}_\times(\tilde{\mathbf{n}}) \cos(2\delta\psi) - \tilde{h}_+(\tilde{\mathbf{n}}) \sin(2\delta\psi). \quad (36b)$$

With respect to the aberrated direction, the strain contains therefore only spin-2 modes, proportional to the spin-2 antenna patterns F_+ and F_\times . Parameter estimations from the GW signal will therefore infer: 1) the aberrated direction \mathbf{n} and 2) the two "mixed" polarisations \hat{h}_+ and \hat{h}_\times . Since the transverse peculiar velocity of the source is unknown, the mixing angle (34) is unknown, and we can therefore not measure the two intrinsic polarisations \tilde{h}_+ and \tilde{h}_\times .

We could wonder if having detectors with arms pointing in different directions could help us break the degeneracy between the source velocity and the true polarisations.

Eq. (35) has indeed been derived in the specific case of a detector with arms pointing in the xy directions. We can show that the degeneracy exists for all cases. At linear order in the velocity, we can indeed rewrite Eqs. (22) and (23) as

$$\begin{aligned} P_{ij} &= \quad (37) \\ &\left[(\tilde{e}_{1i} - v_1 \tilde{n}_i)(\tilde{e}_{1j} - v_1 \tilde{n}_j) - (\tilde{e}_{2i} - v_2 \tilde{n}_i)(\tilde{e}_{2j} - v_2 \tilde{n}_j) \right] \tilde{h}_+ \\ &+ \left[(\tilde{e}_{1i} - v_1 \tilde{n}_i)(\tilde{e}_{2j} - v_2 \tilde{n}_j) + (\tilde{e}_{1j} - v_1 \tilde{n}_j)(\tilde{e}_{2i} - v_2 \tilde{n}_i) \right] \tilde{h}_\times. \end{aligned}$$

We see that, working to linear order in velocity, the boosted dimensionless driving force matrix is equivalent to the one of an unboosted gravitational wave with polarisation axes

$$\mathbf{e}_1 = \tilde{\mathbf{e}}_1 - v_1 \tilde{\mathbf{n}}, \quad (38a)$$

$$\mathbf{e}_2 = \tilde{\mathbf{e}}_2 - v_2 \tilde{\mathbf{n}}. \quad (38b)$$

It is clear that these two polarisation vectors are orthogonal, and they correspond to the polarisation axes of a source coming from direction

$$\mathbf{n} = \mathbf{e}_1 \wedge \mathbf{e}_2 = \tilde{\mathbf{n}} + v_1 \tilde{\mathbf{e}}_1 + v_2 \tilde{\mathbf{e}}_2 = \tilde{\mathbf{n}} + \mathbf{v}_\perp, \quad (39)$$

which is nothing else than the aberrated direction defined in Eq. (30). The polarisation axes \mathbf{e}_1 and \mathbf{e}_2 are not the natural ones associated to the direction \mathbf{n} , as defined in Eqs. (20). We can easily see that the natural axes are related to \mathbf{e}_1 and \mathbf{e}_2 by

$$\hat{\mathbf{e}}_1 = \mathbf{e}_1 - v_1 \frac{\cos\theta}{\sin\theta} \mathbf{e}_2, \quad (40a)$$

$$\hat{\mathbf{e}}_2 = \mathbf{e}_2 + v_1 \frac{\cos\theta}{\sin\theta} \mathbf{e}_1, \quad (40b)$$

This is the infinitesimal form of a rotation in two dimensions

$$\hat{\mathbf{e}}_a = R_a^b \mathbf{e}_b, \quad (41)$$

where the rotation matrix is

$$R_a^b = \begin{pmatrix} \cos(\delta\psi) & \sin(\delta\psi) \\ -\sin(\delta\psi) & \cos(\delta\psi) \end{pmatrix} \simeq \begin{pmatrix} 1 & \delta\psi \\ -\delta\psi & 1 \end{pmatrix}, \quad (42)$$

and $\delta\psi$ is defined in Eq. (34). Inserting Eqs. (40) into Eq. (37) we obtain

$$P_{ij} = \hat{h}_+ (\hat{e}_{1i} \hat{e}_{1j} - \hat{e}_{2i} \hat{e}_{2j}) + \hat{h}_\times (\hat{e}_{1i} \hat{e}_{2j} + \hat{e}_{2i} \hat{e}_{1j}), \quad (43)$$

where \hat{h}_+ and \hat{h}_\times are given by Eqs. (36). From this we see that the response of *any* interferometer can be written in terms of the two standard antenna patterns $F_+(\mathbf{n})$ and $F_\times(\mathbf{n})$ associated to the aberrated direction \mathbf{n} . The two inferred polarisations \hat{h}_+ and \hat{h}_\times are modified by the source velocity.

Eq. (43) tells us that the spin-1 modes that are generated by the velocity of the source can always be re-absorbed into spin-2 modes with aberrated direction \mathbf{n} and mixed polarisations \hat{h}_+ and \hat{h}_\times . One could however wonder if by actively searching for vector modes, i.e. by including spin-1 antenna patterns in the modelling of the signal, one could measure the amplitude of these new modes, as well as the true direction $\tilde{\mathbf{n}}$. This turns out to be impossible, since there is no unique way of splitting the signal into spin-2 modes and spin-1 modes, see Appendix D for details.

As a consequence, from a data analysis point of view, the template of a signal constructed for the direction of propagation $\tilde{\mathbf{n}}$ using spin-2 modes, spin-1 modes and the polarisation angle $\tilde{\Psi}$ will be equivalent (up to a factor $\mathcal{O}(|\mathbf{v}|^2)$)

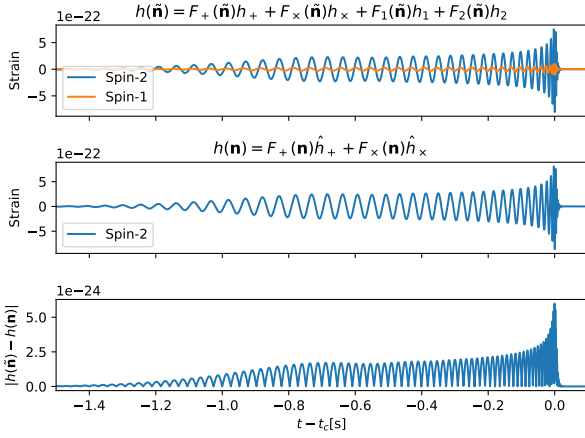


Figure 2. The first and second panels show two templates constructed for a GW signal from a binary with $30M_{\odot} - 30M_{\odot}$ at a distance of 500 Mpc and with $\mathbf{v} = (0.1, 0, 0)$. In the first panel, we construct the template as the sum of two spin-1 (orange line) and spin-2 signals (blue line) using the true sky direction $\tilde{\mathbf{n}}$ and the true polarisation angle $\tilde{\psi}$. In the second panel, we construct the template using the aberrated sky position \mathbf{n} and aberrated polarisation angle ψ and only spin-2 modes. The third panel shows the difference between the two templates which is of the order of $\mathcal{O}(|\mathbf{v}|^2)$, as our framework is defined at the first order in peculiar motion. The detector is taken with arms $\hat{\mathbf{l}} = (1, 0, 0)$ and $\hat{\mathbf{m}} = (0, 1, 0)$.

to the template of a signal propagating in the direction \mathbf{n} with spin-2 modes and polarisation angle Ψ . Fig. 2 shows the templates for the true and the aberrated directions of a simulated GW signal with $|\mathbf{v}| = 0.1$ (see caption for more details). For the true direction, the template is the sum of spin-2 and spin-1 components. As expected, the two templates differ by a factor $\mathcal{O}(|\mathbf{v}|^2)$.

Another manner to understand this total degeneracy is to consider the geometric interpretation of the transformation of the dimensionless driving force matrix from the source frame to the observer frame. Let us consider the rotation vector $\mathcal{A}_{\tilde{\mathbf{n}} \rightarrow \mathbf{n}} = \alpha(\tilde{\mathbf{n}} \wedge \hat{\mathbf{v}}_{\perp})$, where α is the angle between $\tilde{\mathbf{n}}$ and \mathbf{n} and $(\tilde{\mathbf{n}} \wedge \hat{\mathbf{v}}_{\perp})$ is a unit vector orthogonal to them. The rotation around $\mathcal{A}_{\tilde{\mathbf{n}} \rightarrow \mathbf{n}}$ carries $\tilde{\mathbf{n}}$ along a great circle to \mathbf{n} . Its components are

$$R_i^j \equiv \exp\left(-\mathcal{A}_{\tilde{\mathbf{n}} \rightarrow \mathbf{n}}^k \epsilon_{ki}^j\right) \simeq \delta_i^j - \tilde{n}_i v^j + v_i \tilde{n}^j, \quad (44)$$

and the transformation rules (38) are directly seen as the effect of this latter infinitesimal rotation since they are equivalent to $e_{1i} = R_i^j \tilde{e}_{1j}$ and $e_{2i} = R_i^j \tilde{e}_{2j}$. Therefore Eq. (37) is simply

$$P_{ij}(\mathbf{n}) = R_i^p R_j^q \tilde{P}_{pq}(\tilde{\mathbf{n}}), \quad (45)$$

with $\tilde{P}_{ij} = \tilde{h}_{ij}^{\text{TT}}$. We recognize the transformation rule of a tensor on the unit sphere under a rotation R . Hence the driving force matrix is also transformed by the infinitesimal rotation which transports $\tilde{\mathbf{n}}$ onto \mathbf{n} . Note that this transformation is equivalent to a parallel transport of the driving force along the great circle connecting $\tilde{\mathbf{n}}$ and \mathbf{n} , as by construction both vectors lie in the equatorial plane of vectors normal to $\mathcal{A}_{\tilde{\mathbf{n}} \rightarrow \mathbf{n}}$.

However, even though in the source frame we chose for

convenience to use the vectors naturally associated with the spherical components (Eqs. (20b) and (20c)), the rotated ones, \mathbf{e}_1 and \mathbf{e}_2 , are not directly the unit vectors naturally associated with spherical coordinates in the observer frame: $\hat{\mathbf{e}}_1$ and $\hat{\mathbf{e}}_2$. Both sets being orthonormal and normal to \mathbf{n} , they are related by a rotation around \mathbf{n} of angle $\delta\psi$, that is Eq. (41), with R_a^b related to R_i^j through $R_a^b \equiv \hat{e}_a^i e_{bi} = \hat{e}_a^i R_i^j \tilde{e}_{bj}$.

Therefore, from the simple transformation rule (45), the spherical basis components of the driving force, which are $\tilde{P}_{ab} \equiv \tilde{e}_a^i \tilde{e}_b^j \tilde{P}_{ij}$ and $P_{ab} \equiv \hat{e}_a^i \hat{e}_b^j P_{ij}$, are related through

$$P_{ab}(\mathbf{n}) = R_a^c R_b^d \tilde{P}_{cd}(\tilde{\mathbf{n}}). \quad (46)$$

This is yet another way to write the transformation rule of a tensor on the unit sphere under a rotation, which translates into Eqs. (36) for the polarisation components. In short, the mixing of polarisations is essentially a consequence of the fact that the basis used to define polarisations, the natural spherical basis, is not parallel transported along the great circle connecting $\tilde{\mathbf{n}}$ to \mathbf{n} , whereas the driving force matrix is parallel transported. The only exception is when the great circle connecting $\tilde{\mathbf{n}}$ to \mathbf{n} is either the equator or a meridian of the spherical coordinates system. For infinitesimal transformations which we have considered here, the natural spherical basis is also (infinitesimally) parallel transported whenever the direction (initial or final, this is equivalent for infinitesimal transformations) is on the equator, even if the transformation direction is not tangential to the equator. That is whenever the conditions $\theta = \pi/2$ (emitting direction on the equator) or $v_1 = 0$ (an aberration along a meridian) are satisfied, the natural spherical basis is infinitesimally parallel transported, and we can check that indeed $\delta\psi = 0$ under these conditions.

Also, one should bear in mind that the rotation (44) which accounts for the effect of the transverse velocity depends on $\tilde{\mathbf{n}}$ and is not a unique global rotation. Therefore, a source with a transverse velocity is degenerate from a source without velocity but rotated with R , only because we can observe a single emission direction. Finally, let us highlight that the transformation of the driving force matrix due to a transverse velocity, seen as rotation or as parallel transport, is similar to the transformation of the CMB polarisation tensor which is also a spin-2 quantity, see e.g. Section III of Challinor & van Leeuwen (2002).

5 TIME DELAY FROM A NETWORK OF DETECTORS

For a network of interferometers, in addition to the signal measured by each detector, the time delay between the different detectors due to their different position with respect to the source is measured. This time delay depends directly on the direction of the source, and provides therefore a precise way of measuring this direction (more precise than from the antenna patterns, since the phase of the GW is measured with a better precision than the amplitude of the two polarisations). We will see that in the case of a moving source the time delay depends on the aberrated direction \mathbf{n} and not on the true direction $\tilde{\mathbf{n}}$.

We consider the geometry plotted in Fig. 3. In the reference frame of the source (denoted by tilde), the source emits

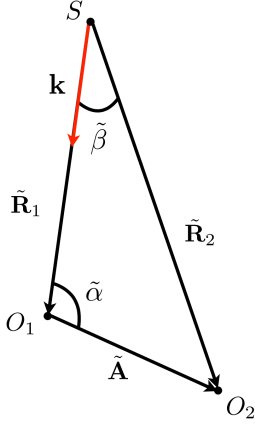


Figure 3. Geometrical configuration used to calculate the time delay.

a GW at time $\tilde{t}_e = 0$ and at position $\tilde{\mathbf{R}}_e = (0, 0, 0)$. The first interferometer receives the wave at time \tilde{t}_1 and position $\tilde{\mathbf{R}}_1$, where $\tilde{R}_1 = \tilde{t}_1$ (let us recall that we work in units $c = 1$). The observer, who is moving with a velocity $-\mathbf{v}$ with respect to the source, sees boosted coordinates $x_\mu = (t, \mathbf{R}) = \Lambda_\mu^\nu \tilde{x}_\nu$, where Λ is defined in Appendix A. At linear order in the velocity the time of emission and reception are given by

$$t_e = \tilde{t}_e + \mathbf{v} \cdot \tilde{\mathbf{R}}_e = 0, \quad (47a)$$

$$t_1 = \tilde{t}_1 + \mathbf{v} \cdot \tilde{\mathbf{R}}_1 = \tilde{R}_1 + \mathbf{v} \cdot \tilde{\mathbf{R}}_1. \quad (47b)$$

The same calculation applies to the second interferometer. The difference in arrival time between the two detectors is therefore given by

$$\Delta t \equiv t_2 - t_1 = \tilde{R}_2 - \tilde{R}_1 + \mathbf{v} \cdot (\tilde{\mathbf{R}}_2 - \tilde{\mathbf{R}}_1). \quad (48)$$

Defining $\tilde{\mathbf{A}}$ as the vector connecting the two detectors:

$$\tilde{\mathbf{A}} = \tilde{\mathbf{R}}_2 - \tilde{\mathbf{R}}_1, \quad (49)$$

we see from Fig. 3 that

$$\tilde{A}^2 = \tilde{R}_1^2 + \tilde{R}_2^2 - 2\tilde{R}_1\tilde{R}_2 \cos \tilde{\beta}, \quad (50a)$$

$$\tilde{R}_2^2 = \tilde{R}_1^2 + \tilde{A}^2 - 2\tilde{R}_1\tilde{A} \cos \tilde{\alpha}, \quad (50b)$$

leading to

$$\tilde{R}_2 \cos \tilde{\alpha} - \tilde{R}_1 = -\tilde{A} \cos \tilde{\alpha} = \tilde{\mathbf{A}} \cdot \tilde{\mathbf{n}}. \quad (51)$$

We are interested in situations where the distance to the source is much larger than the distance between the detectors, such that $\cos \tilde{\beta} \simeq 1$. The time delay becomes then

$$\Delta t = \tilde{\mathbf{A}} \cdot (\tilde{\mathbf{n}} + \mathbf{v}). \quad (52)$$

The distance between the two detectors in the source frame, $\tilde{\mathbf{A}}$, can be related to the distance in the observer frame using that

$$\tilde{R}_{1i} = (\Lambda^{-1})_i^\mu x_{1\mu} = -v_i t_1 + R_{1i}, \quad (53)$$

and similarly for \tilde{R}_{2i} . This leads to

$$\tilde{\mathbf{A}} = \mathbf{A} - \mathbf{v} \cdot \Delta t. \quad (54)$$

Inserting this in Eq. (52) and keeping only terms at linear order in the velocity we obtain

$$\Delta t = \mathbf{A} \cdot (\tilde{\mathbf{n}} + \mathbf{v} - v_3 \tilde{\mathbf{n}}) = \mathbf{A} \cdot (\tilde{\mathbf{n}} + \mathbf{v}_\perp) = \mathbf{A} \cdot \mathbf{n}. \quad (55)$$

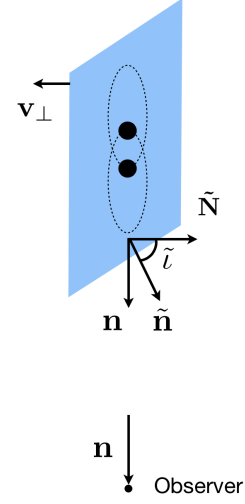


Figure 4. Sketch of the effect of aberration for a binary which is edge-on with respect to the observer.

The time delay is therefore proportional to the aberrated direction \mathbf{n} .

In practice, one often measures the phase shift between the waveform detected by two detectors at a fixed reference time, rather than the time delay. We can easily show that the phase shift is affected in the same way as the time delay by the source velocity. The phases at time t and positions \mathbf{R}_1 and \mathbf{R}_2 are given by

$$\Phi(t, \mathbf{R}_1) = -k^\mu x_{\mu 1} = E(t - \mathbf{R}_1 \cdot \mathbf{n}), \quad (56a)$$

$$\Phi(t, \mathbf{R}_2) = -k^\mu x_{\mu 2} = E(t - \mathbf{R}_2 \cdot \mathbf{n}), \quad (56b)$$

where $k^\mu = E(-1, \mathbf{n})$. The phase shift is given by

$$\Delta\Phi = -E \mathbf{A} \cdot \mathbf{n}. \quad (57)$$

As expected, the phase shift is therefore also proportional to the aberrated direction \mathbf{n} .

This calculation of the time delay (and the phase shift) shows that a network of detectors also measures the aberrated direction and not the intrinsic one in the source frame.

6 OBSERVATIONAL IMPACT OF THE SOURCE VELOCITY

We have seen that the source velocity affects the strain in two ways: 1) it aberrates the direction of the source, both in the antenna patterns and in the time delay; and 2) it mixes the two polarisations of the wave. The first effect is common to any signal emitted by a moving source. In particular it affects in the exact same way electromagnetic signals. The second effect on the other hand is specific to the fact that a GW is a spinned quantity. This effect is therefore absent in standard optical or radio surveys, where we measure the intensity (which is a spin-zero quantity) of the electromagnetic field.³ These two effects have a direct impact on the measurement of the parameters of the binary.

As for electromagnetic signals, aberration means that

³ It would however be present if we were to measure directly the electromagnetic field, which is a spin-1 quantity.

we do not receive the GW that have been emitted in the observed direction \mathbf{n} , but rather the GW that have been emitted in a different direction $\tilde{\mathbf{n}}$. As depicted in Fig. 4, the source appears therefore in the correct position, but the form of the wave corresponds to the one emitted in direction $\tilde{\mathbf{n}}$. Since GW are not isotropically emitted by the binary system, aberration has a direct impact on the amplitude of the detected signal. In particular, even though the signal seems to come from direction \mathbf{n} , the inclination angle that governs the amplitude of the signal is the one associated to the direction $\tilde{\mathbf{n}}$. The relation between $\tilde{\iota}$, defined as the angle between $\tilde{\mathbf{n}}$ and the normal to the plane of the binary in the frame of the source $\tilde{\mathbf{N}}$ (see Fig. 4), and the true inclination angle ι that we would have if there would be no velocity (i.e. the angle between \mathbf{n} and $\tilde{\mathbf{n}}$) directly follows from the relation between \mathbf{n} and $\tilde{\mathbf{n}}$ and is therefore linear in the transverse velocity \mathbf{v}_\perp . The polarisations \tilde{h}_+ and \tilde{h}_\times in Eqs. (36) depend however not directly on $\tilde{\iota}$ but on its cosine, which is related to the one in absence of velocity by

$$\cos \tilde{\iota} = \cos \iota - \tilde{\mathbf{N}} \cdot \mathbf{v}_\perp. \quad (58)$$

We see that the effect vanishes for a binary that is face-on, since in this case $\tilde{\mathbf{N}}$ is parallel to \mathbf{n} , which is perpendicular to \mathbf{v}_\perp (note that this does not hold at higher order in the velocity). On the contrary the effect is maximum for a binary which is edge-on, and with \mathbf{v}_\perp orthogonal to the plane of the binary, as illustrated in Fig. 4. The fact that the amplitude of the effect depends on $\tilde{\mathbf{N}}$, i.e. on the orientation of the plane with respect to the observer, is directly linked to the fact that the amplitude of the polarisations scales with $\cos \tilde{\iota}$. For $\iota = 0$, the change is quadratic in $\delta\iota$: $\cos(\tilde{\iota}) = \cos(0 + \delta\iota) \simeq 1 - \delta\iota^2/2$, whereas for $\iota = \pi/2$ the change is linear: $\cos(\tilde{\iota}) = \cos(\pi/2 + \delta\iota) \simeq -\delta\iota$.

In Fig. 4 we show for illustration the case where the effect of aberration is maximum. In this configuration, if the source were not moving, we would receive only the h_+ polarisation, since only h_+ is emitted along \mathbf{n} ($\cos \iota = 0$ meaning that $h_\times = 0$). However, since the source is moving, we do not receive the GWs that have been emitted in direction \mathbf{n} but rather the GWs that have been emitted in direction $\tilde{\mathbf{n}}$ (and that we see coming from direction \mathbf{n}). Along $\tilde{\mathbf{n}}$ both h_+ and h_\times are produced and therefore we observe these two polarisations. From this we wrongly conclude that the plane of the binary is slightly inclined with respect to us, i.e. that the binary is not edge-on.

The second effect, the mixing of polarisations, simply means that the true polarisation of the source cannot be inferred, but that one measures instead a wrong polarisation

$$\Psi = \tilde{\Psi} - v_1 \frac{\cos \theta}{\sin \theta}. \quad (59)$$

Like for aberration, this means that the plane of the binary appears slightly turned (this time around \mathbf{n}) with respect to the observer.

We see therefore that the source velocity biases the measurement of the angles describing the orientation of the binary system with respect to the observer. However, since these intrinsic parameters are unknown and randomly distributed over the population of sources, having a wrong measurement of them has no direct observational impact. In particular, the other parameters like the luminosity distance and the chirp mass are not affected by aberration and by the

change in polarisation, since the source velocity is fully reabsorbed into the new direction \mathbf{n} and the new polarisation Ψ . This can be mathematically seen with the Fisher formalism. The measured strain h depends on a set of parameters Θ . The Fisher matrix associated to these parameters is given by

$$\Gamma^{ij} = \left(\frac{\partial h(\Theta)}{\partial \Theta_i} \middle| \frac{\partial h(\Theta)}{\partial \Theta_j} \right) \quad (60)$$

where the scalar product is defined as

$$(a|b) = 4\mathcal{R}e \left[\int_{f_{\text{low}}}^{f_{\text{high}}} \frac{\hat{a}(f)^* \hat{b}(f)}{S(f)} df \right], \quad (61)$$

where $S(f)$ is the detector power spectral density (PSD), f is the GW frequency, $*$ indicates the complex conjugate, $\hat{\cdot}$ the Fourier components, f_{low} is a low frequency cut-off given by the detector sensitivity and f_{high} an high frequency cut-off given by the sampling rate of data. The bias induced on the parameters Θ by the source velocity is then given by

$$\Delta \Theta^i = (\Gamma^{-1})^{ij} \left(\frac{\partial h(\Theta)}{\partial \Theta_j} \middle| h(\Theta) - \tilde{h}(\Theta) \right), \quad (62)$$

where \tilde{h} is the strain that we would have in the absence of velocity. In our case, the difference between h and \tilde{h} can be fully reabsorbed into a different polarisation and different inclination angle. The observed strain (35) is found from the transformation rules (36) which are equivalent to (46), that is to a rotation of the source with R . Hence we can write that $\tilde{h}(\Theta) = h(R^{-1}(\Theta))$, where $R^{-1}(\Theta)$ are the parameters characterising a source with initial parameters Θ and subsequently rotated with R^{-1} . That is, if Θ defines a binary plane orthogonal to N_i , then $R^{-1}(\Theta)$ defines a rotated binary plane orthogonal to $R_i^{-1j} N_j$. Defining the parameters shifts by $\delta\Theta = \Theta - R^{-1}(\Theta)$, the only non-zero components of $\delta\Theta$ are $\delta\Psi$ and $\delta(\cos \iota)$ since they characterise the orientation of the binary plane. Taylor expanding around Θ we then obtain

$$\tilde{h}(\Theta) \simeq h(\Theta) - \frac{\partial h(\Theta)}{\partial \Theta^k} \delta\Theta^k, \quad (63)$$

leading to

$$\begin{aligned} \Delta \Theta^i &= (\Gamma^{-1})^{ij} \left(\frac{\partial h(\Theta)}{\partial \Theta_j} \middle| \frac{\partial h(\Theta)}{\partial \Theta_k} \right) \delta\Theta^k \\ &= (\Gamma^{-1})^{ij} \Gamma_{jk} \delta\Theta^k = \delta\Theta^i. \end{aligned} \quad (64)$$

Hence we see that the only parameters that are biased by the transverse velocity of the source are the polarisation and the inclination angle. In particular, the source transverse velocity has no impact on the luminosity distance and the chirp mass.

Let us conclude this section by noting that while the difference between \mathbf{n} and $\tilde{\mathbf{n}}$ depends on the relative velocity between the source and the observer and is therefore the same if the source moves with velocity \mathbf{v}_\perp with respect to the observer or if the observer moves with velocity $-\mathbf{v}_\perp$ with respect to the source, the observational consequences are different in these two cases. In the case of a moving source, the incoming direction of the GW in the observer frame is not affected by the motion. As a consequence \mathbf{n} denotes the true direction of the source, and $\tilde{\mathbf{n}}$ is the direction of emission in the source frame, as depicted in Fig. 4. The source velocities

have therefore no impact on the observed position of sources in the sky. The velocity only affects the part of the source that the observer sees. On the other hand, in the case of a moving observer, the emitted direction of the GW in the source frame is not affected by the motion. Consequently $\hat{\mathbf{n}}$ denotes the true direction of the source, and \mathbf{n} the apparent direction, seen by the moving observer. The observed positions of sources in the sky are therefore affected by the observer velocity. More precisely, the observer velocity with respect to a frame where sources are on average at rest generates a dipole in the source distribution, as computed for example in [Mastrogiovanni et al. \(2022\)](#) for GW events or in [Domènech et al. \(2022\)](#) and [Dalang et al. \(2022\)](#) for galaxy counts.

7 CONCLUSIONS

In this paper, we showed that the peculiar motion of a gravitational wave source with respect to the observer rest frame, induces a distortion in the observed waveform. In particular the presence of a (non-zero) component of the peculiar velocity transverse to the line-of-sight gives rise to apparent vector polarisations in the observer frame. These are pure projection effects, proportional to the plus and cross polarisations in the source frame. They share therefore the same time dependence as the spin-2 modes and do not correspond to new degrees of freedom. We have shown that this implies that the spin-1 modes can always be rewritten as spin-2 modes coming from an aberrated direction, and with a slightly different polarisation.

One could however wonder if by actively searching for vector modes, i.e. by including spin-1 antenna patterns in the modeling of the strain, one could measure the amplitude of these new modes, as well as the true (non aberrated) source location. Comparing this with the aberrated direction obtained from the time-delay, one could then measure the transverse velocity. We showed that unfortunately, this is not feasible since, without knowing the peculiar velocity, there is no unique/preferred way of splitting the signal into spin-2 modes and spin-1 modes. The only meaningful solution is therefore the one with no spin-1 mode. This is indeed the only solution for which the direction inferred from the waveform and the direction inferred from time delay are the same.

A direct consequence of the aberration of GW sources is that the parameters encoding the orientation of the binary system with respect to the observer are biased. For example, a binary that is edge-on, for which we should only detect a h_+ polarisation, will appear slightly inclined since we will receive both h_+ and h_\times polarisations. The inclination angle and the polarisation angle that we measure are therefore not the true ones. Since these angles are unknown and are independent of other parameters, like the chirp mass or the luminosity distance, this bias has no direct impact on astrophysical or cosmological constraints inferred from GW measurements such as [Finke et al. \(2021\)](#); [Leyde et al. \(2022\)](#); [The LIGO Scientific Collaboration et al. \(2021b\)](#); [Mancarella et al. \(2022\)](#); [Iacovelli et al. \(2022\)](#). However, it might impact studies aiming at constraining the inclination distribution of binaries ([Vitale et al. 2022](#)).

We stress that the same effect is present in the case of

an astrophysical source emitting spin-1 waves: if we look at the electric field emitted by such a source we find that the direction of propagation of the spin-1 wave is aberrated and that the only effect on the source parameters is an apparent rotation (i.e. the intrinsic angles defining the source orientation are biased). For example, for gamma-ray burst sources, if one defines an angle ι between the line of sight and the normal to the rotation plane, the effect of a transverse velocity is given by a change in the source orientation due to aberration given by Eq. (58), and a mixing of the two spin-1 polarisations of the emitted electromagnetic radiation.

We observe that our findings significantly differ from the conclusions of [Torres-Orjuela et al. \(2019\)](#). The authors of this reference compute distortions in the antenna pattern function of a GW detector, induced by a peculiar motion of the observer frame with respect to the frame of emission. They find that a velocity component orthogonal to the line of sight gives a non-monotonic modification of the amplitude of the wave. However, while the authors consider kinematic effects on the source position, they neglect the effect induced by a relative motion on the directions of GW polarisation (they defer this study to a future work). It is likely that by properly accounting for this change, they would find that the modifications in the antenna pattern can be reabsorbed into a redefinition of the propagation direction (in agreement with our results). This has a profound impact on the resulting signal. Indeed, contrary to what is concluded in [Torres-Orjuela et al. \(2019\)](#), we find that the impact of transverse velocities on GWs is completely analogous to the one on electromagnetic signals, i.e. it can be fully explained in terms of a relativistic beaming effect without the need of invoking additional corrections. We also find that transverse velocities do not produce spurious non-GR-like signals nor modifications in the source luminosity distance, unlike what is claimed in that reference.

In [Torres-Orjuela et al. \(2021\)](#) the authors claim that when considering aberration and polarisation rotation, not only the frequency of the GWs change but also the amplitude of their spherical modes. They deduce that this allows the detection of the transverse speed of a source (i.e. the authors claim that the effect cannot be reabsorbed into a redefinition of the source's intrinsic orientation). This is in direct contradiction with what we have shown explicitly in this article. Their proof is based on the determination of the transformation matrix which relates multipoles in the source frame to multipoles in the observer frame. Their Eq. (37) can be seen as such a transformation when using a multi-index notation $L = (\ell, m)$, as it is of the form $\sum_L \mathcal{Y}_K^L H^L = H'^K$, with \mathcal{Y}_K^L a matrix. They then deduce that their Eq. (39) leads to a contradiction to the existence of such a matrix, whereas in fact it simply determines the coefficients in one line of the transformation matrix \mathcal{Y}_K^L when $L = (2, 2)$. Note that the problem of finding how the multipoles of a signal are transformed by a boost, that is finding the \mathcal{Y}_K^L , has already been solved for spin-0 and spin-2 quantities in the context of CMB temperature and polarisation in e.g. [Challinor & van Leeuwen \(2002\)](#), [Dai & Chluba \(2014\)](#) and [Yasini & Pierpaoli \(2017\)](#). In any case, the crucial point is that since we are observing from a single position, we cannot see the change in the multipoles due to the source velocity. We can only sample the GW field in one direction, and as we have demonstrated in this paper, the boosted field in one direc-

tion is fully degenerate with the unboosted one in a different direction.

We conclude with a final remark: one might be tempted to assume that the large-scale correlations of the (cosmic-flow) velocity across the sky would induce correlations between the inclination angle of different sources. Measuring such a correlation, would then provide a direct way of measuring the transverse cosmological velocity. Unfortunately, the correlation of inclination angle turns out to be always vanishing: the change in inclination $\delta\iota = \tilde{\iota} - \iota$ does not depend directly on the transverse velocity \mathbf{v}_\perp but on the projection of \mathbf{v}_\perp on a random variable $\tilde{\mathbf{N}}$. This completely removes the correlation (see Appendix E for details). We stress that even if we would correlate $\cos\iota$ with another quantity, e.g. galaxy number density, the correlation would also vanish. Aberration can therefore not be used to measure the transverse velocity of sources.

ACKNOWLEDGEMENT

We thank Nicola Tamanini for interesting discussions and exchanges. We also thank Ruth Durrer for valuable discussions and feedback during the early stage of this project. C. B. acknowledges support from the Swiss National Science Foundation and from the European Research Council (ERC) under the European Union's Horizon 2020 research and innovation program (Grant agreement No. 863929; project title "Testing the law of gravity with novel large-scale structure observables"). The work of G. Cu. is funded by Swiss National Science Foundation (Ambizione grant *Gravitational wave propagation in the clustered universe*) and by CNRS. For the purpose of open access, the authors have applied a Creative Commons Attribution (CC BY) licence to any Author Accepted Manuscript version arising from this submission.

APPENDIX A: TRANSFORMATIONS OF THE METRIC TENSOR

We now consider how metric perturbation in 4 dimensions transforms under boost of velocity $-\mathbf{v}$ (since the observer moves with velocity $-\mathbf{v}$ with respect to the source). The metric perturbation transforms as

$$\begin{aligned} h_{\mu\nu} &= \Lambda_\mu^\alpha \Lambda_\nu^\beta \tilde{h}_{\alpha\beta}, \\ h^{\mu\nu} &= \Lambda^\mu_\alpha \Lambda^\nu_\beta \tilde{h}^{\alpha\beta}, \end{aligned} \quad (\text{A1})$$

where

$$\begin{aligned} \Lambda^0_0 &= \gamma, & \Lambda^0_i &= \Lambda^i_0 = -\gamma v_i, \\ \Lambda^i_j &= \delta^i_j + \frac{\gamma^2}{1+\gamma} v^i v^j, \\ \Lambda_0^0 &= \gamma, & \Lambda_0^i &= \Lambda_i^0 = \gamma v^i, \\ \Lambda_i^j &= \delta_i^j + \frac{\gamma^2}{1+\gamma} v_i v^j, \end{aligned} \quad (\text{A2})$$

with $\gamma^{-2} = 1 - v_i v^i$ and $\beta^2 \equiv v_i v^i$.

Let us start with upper indices

$$\begin{aligned} h^{00} &= \Lambda^0_\alpha \Lambda^0_\beta \tilde{h}^{\alpha\beta}, \\ h^{0i} &= \Lambda^0_\alpha \Lambda^i_\beta \tilde{h}^{\alpha\beta}, \\ h^{ij} &= \Lambda^j_\alpha \Lambda^i_\beta \tilde{h}^{\alpha\beta}. \end{aligned} \quad (\text{A3})$$

Now we assume that in the non-tilde frame (frame comoving with the source) we are in TT gauge, implying $\tilde{h}^{00} = \tilde{h}^{0i} = 0$.

$$\begin{aligned} h^{00} &= \Lambda^0_m \Lambda^0_n \tilde{h}^{mn} = \gamma^2 v_m v_n \tilde{h}^{mn}, \\ h^{0i} &= \Lambda^0_m \Lambda^i_n \tilde{h}^{mn} = -\gamma v_m \left(\delta_n^i + \frac{\gamma^2}{1+\gamma} v^i v_n \right) \tilde{h}^{mn}, \\ h^{ij} &= \Lambda^i_m \Lambda^j_n \tilde{h}^{mn} \\ &= \left(\delta_m^i + \frac{\gamma^2}{1+\gamma} v^i v_m \right) \left(\delta_n^j + \frac{\gamma^2}{1+\gamma} v^j v_n \right) \tilde{h}^{mn}. \end{aligned} \quad (\text{A4})$$

At linear order in the velocity

$$\begin{aligned} h^{00} &= 0, \\ h^{0i} &= -v_m \tilde{h}^{mi}, \\ h^{ij} &= \tilde{h}^{ij}. \end{aligned} \quad (\text{A5})$$

In flat space it follows that

$$\begin{aligned} h_{00} &= 0, \\ h_{0i} &= v_m \tilde{h}_{mi}, \\ h_{ij} &= \tilde{h}_{ij}. \end{aligned} \quad (\text{A6})$$

The wave in the observer frame (without a tilde) is not in the TT gauge anymore. However, it is possible to fix the TT gauge with respect to the observer by performing the set of transformations detailed in the next appendix.

APPENDIX B: GAUGE TRANSFORMATION TO PURELY SPATIAL PERTURBATION

Suppose we have a general plane gravitational wave of the form

$$h_{ab} = H_{ab} f(k^a x_a) \quad \text{with} \quad k^a k_a = 0.$$

Without loss of generality we choose spatial axes such that the gravitational wave is propagating in the \hat{z} direction, so that $\hat{k}_a = (1, 0, 0, 1)$. We now consider a gauge transformation of the form

$$\xi^a = \Xi^a F(k^a x_a), \quad (\text{B1})$$

where $F(u)$ is the integral of $f(u)$, i.e., $dF/du = f(u)$. A gauge transformation of this form leads to a transformation of the metric perturbation

$$\begin{aligned} h_{ab}^{\text{new}} &= h_{ab}^{\text{old}} - \partial_a \xi_b - \partial_b \xi_a \\ &= H_{ab}^{\text{new}} f(k^a x_a), \end{aligned} \quad (\text{B2})$$

in which

$$H_{ab}^{\text{new}} = H_{ab} - \begin{pmatrix} 2\Xi_0 & \Xi_x & \Xi_y & \Xi_z + \Xi_0 \\ \Xi_x & 0 & 0 & \Xi_x \\ \Xi_y & 0 & 0 & \Xi_y \\ \Xi_z + \Xi_0 & \Xi_x & \Xi_y & 2\Xi_z \end{pmatrix}. \quad (\text{B3})$$

Making the choice

$$\Xi_a = \left(\frac{1}{2} H_{00}, H_{0x}, H_{0y}, -\frac{1}{2} H_{00} + H_{0z} \right) \quad (\text{B4})$$

reduces the metric perturbation to purely spatial form

$$H_{ab}^{\text{new}} = \begin{pmatrix} 0 & 0 & 0 & 0 \\ 0 & H_{xx} & H_{xy} & -H_{0x} \\ 0 & H_{xy} & H_{yy} & -H_{0y} \\ 0 & -H_{0x} & -H_{0y} & H_{zz} + H_{00} - 2H_{0z} \end{pmatrix}. \quad (\text{B5})$$

For the particular metric components given in Eq. (A6), this gauge transformation gives

$$H_{ab}^{\text{new}} = \begin{pmatrix} 0 & 0 & 0 & 0 \\ 0 & \tilde{h}_{xx} & \tilde{h}_{xy} & -v_x \tilde{h}_{xx} - v_y \tilde{h}_{xy} \\ 0 & \tilde{h}_{xy} & \tilde{h}_{yy} & -v_x \tilde{h}_{xy} + v_y \tilde{h}_{xx} \\ 0 & -v_x \tilde{h}_{xx} - v_y \tilde{h}_{xy} & v_y \tilde{h}_{xx} - v_x \tilde{h}_{xy} & 0 \end{pmatrix} \quad (\text{B6})$$

in which we have used $\tilde{h}_{yy} = -\tilde{h}_{xx}$ and $\tilde{h}_{00} = \tilde{h}_{0z} = \tilde{h}_{zz} = 0$. We see that this gauge transformation makes the purely spatial part of the metric equal to the electric components of the Riemann tensor, justifying the assumptions made in Section 3.2.

APPENDIX C: RELATION BETWEEN PROPER TIMES

To relate the proper time in the source frame $d\tilde{\tau}$ to the proper time in the observer frame $d\tau$, we proceed in the following way. We first relate the 4-momentum of the GW in the source and observer frame to the phase Φ ⁴

$$\tilde{k}_\mu = -\frac{\partial}{\partial \tilde{x}^\mu} \Phi \quad (\text{C1})$$

$$k_\mu = -\frac{\partial}{\partial x^\mu} \Phi. \quad (\text{C2})$$

⁴ Since Φ is a scalar, it is invariant under a boost: $\tilde{\Phi} = \Phi$.

Since GWs propagate along null geodesics, the phase is conserved during propagation:

$$\tilde{k}^\mu \tilde{k}_\mu = -\tilde{k}^\mu \frac{\partial}{\partial \tilde{x}^\mu} \Phi = 0. \quad (\text{C3})$$

Let us now consider two GWs emitted subsequently: the first one at time $\tilde{\tau}$ with phase $\Phi(\tilde{\tau})$ and the second one at time $\tilde{\tau} + d\tilde{\tau}$ with phase $\Phi(\tilde{\tau} + d\tilde{\tau})$. The observer receives these GWs at time τ and $\tau + d\tau$ respectively and since the phase is conserved we have

$$\Phi(\tilde{\tau} + d\tilde{\tau}) - \Phi(\tilde{\tau}) = \Phi(\tau + d\tau) - \Phi(\tau). \quad (\text{C4})$$

Using that

$$\Phi(\tilde{\tau} + d\tilde{\tau}) - \Phi(\tilde{\tau}) = d\tilde{\tau} \frac{d\Phi}{d\tilde{\tau}} = d\tilde{\tau} \tilde{u}^\alpha \frac{\partial \Phi}{\partial \tilde{x}^\alpha} = d\tilde{\tau} \tilde{u}^\alpha \tilde{k}_\alpha = -\tilde{E} d\tilde{\tau}, \quad (\text{C5})$$

and similarly at the observer, we find

$$\tilde{E} d\tilde{\tau} = E d\tau. \quad (\text{C6})$$

APPENDIX D: VECTOR AND TENSOR MODE SPLITTING

One could wonder if by actively searching for vector modes, i.e. by including spin-1 antenna patterns in the modelling of the signal, one could measure the amplitude of these new modes, as well as the true direction $\tilde{\mathbf{n}}$. Comparing this with the aberrated direction obtained from the time-delay, one could then measure the transverse velocity \mathbf{v}_\perp . We show here that this turns out to be impossible, since there is no unique way of splitting the signal into spin-2 modes and spin-1 modes.

We start from the dimensionless driving force matrix computed in Eq. (22) and we split the transverse velocity of the source as

$$\mathbf{v}_\perp = (\mathbf{v}_\perp - \mathbf{w}_\perp) + \mathbf{w}_\perp, \quad (\text{D1})$$

where \mathbf{w}_\perp is an arbitrary transverse velocity with amplitude $w_\perp \ll 1$ such that we can work at linear order in the velocities. The aberrated direction related to the transverse velocity \mathbf{w}_\perp is given by

$$\mathbf{s} = \tilde{\mathbf{n}} + w_1 \tilde{\mathbf{e}}_1 + w_2 \tilde{\mathbf{e}}_2. \quad (\text{D2})$$

Following Eqs. (38) we define the two natural polarisation axes associated to \mathbf{s} :

$$\hat{\mathbf{f}}_1 = \tilde{\mathbf{e}}_1 - w_1 \tilde{\mathbf{n}} - w_1 \frac{\cos \tilde{\theta}}{\sin \tilde{\theta}} \tilde{\mathbf{e}}_2, \quad (\text{D3a})$$

$$\hat{\mathbf{f}}_2 = \tilde{\mathbf{e}}_2 - w_2 \tilde{\mathbf{n}} + w_1 \frac{\cos \tilde{\theta}}{\sin \tilde{\theta}} \tilde{\mathbf{e}}_1. \quad (\text{D3b})$$

Inserting this into (22) we find for the dimensionless driving force matrix

$$\begin{aligned} P_{ij} &= \hat{H}_+ (\hat{f}_{1i} \hat{f}_{1j} - \hat{f}_{2i} \hat{f}_{2j}) + \hat{H}_\times (\hat{f}_{1i} \hat{f}_{2j} + \hat{f}_{2i} \hat{f}_{1j}) \\ &\quad + \hat{H}_1 (s_i \hat{f}_{1j} + \hat{f}_{1i} s_j) + \hat{H}_2 (s_i \hat{f}_{2j} + \hat{f}_{2i} s_j), \end{aligned} \quad (\text{D4})$$

where

$$\hat{H}_+ = \tilde{h}_+ - 2w_1 \frac{\cos \tilde{\theta}}{\sin \tilde{\theta}} \tilde{h}_\times, \quad (\text{D5a})$$

$$\hat{H}_\times = \tilde{h}_\times + 2w_1 \frac{\cos \tilde{\theta}}{\sin \tilde{\theta}} \tilde{h}_+, \quad (\text{D5b})$$

$$\hat{H}_1 = -(v_1 - w_1)\tilde{h}_+ - (v_2 - w_2)\tilde{h}_\times, \quad (\text{D5c})$$

$$\hat{H}_2 = -(v_1 - w_1)\tilde{h}_\times + (v_2 - w_2)\tilde{h}_+. \quad (\text{D5d})$$

From this we see that there is an infinite number of ways of splitting the signal into spin-2 and spin-1 modes with associated aberrated direction \mathbf{s} . There is no way to determine which splitting corresponds to the true velocity \mathbf{v} and therefore the only meaningful solution is the one with no spin-1 modes. This is indeed the only solution for which the direction inferred from the waveform and the direction inferred from time delay are the same.

APPENDIX E: ZERO CORRELATION OF ORIENTATION ACROSS THE SKY

In this appendix we schematically prove that the 2-point correlation function of the source orientation across the sky is vanishing. We assume to have two pixels across the sky, each one containing a set of GW binary systems, with random orientations \tilde{N}_1^i in the first pixel and \tilde{N}_2^j in the second one.

When we correlate two different pixels in the sky we get

$$\begin{aligned} \langle \cos \tilde{\iota}_1 \cos \tilde{\iota}_2 \rangle &= -\langle \cos \iota_1 \tilde{\mathbf{N}}_2 \cdot \mathbf{v}_\perp^1 \rangle - \langle \cos \iota_2 \tilde{\mathbf{N}}_2 \cdot \mathbf{v}_\perp^1 \rangle \\ &+ \langle \cos \iota_1 \cos \iota_2 \rangle + \langle \tilde{\mathbf{N}}_1 \cdot \mathbf{v}_\perp^1 \tilde{\mathbf{N}}_2 \cdot \mathbf{v}_\perp^1 \rangle, \end{aligned} \quad (\text{E1})$$

where the mean has to be interpreted as an ensemble average when acting on stochastic velocities and as a geometric mean over a bunch of sources when acting on geometric quantities. This can be rewritten as

$$\begin{aligned} \langle \cos \tilde{\iota}_1 \cos \tilde{\iota}_2 \rangle &= -\langle \cos \iota_1 \rangle \langle \tilde{\mathbf{N}}_2 \cdot \mathbf{v}_\perp^1 \rangle - \langle \cos \iota_2 \rangle \langle \tilde{\mathbf{N}}_2 \cdot \mathbf{v}_\perp^1 \rangle \\ &+ \langle \cos \iota_1 \rangle \langle \cos \iota_2 \rangle + \langle \tilde{N}_1^i \tilde{N}_2^j \rangle \langle v_{\perp i}^1 v_{\perp j}^1 \rangle. \end{aligned} \quad (\text{E2})$$

It is apparent that the first three terms on the right hand side vanish. However the last vanishes as well due to

$$\langle \tilde{N}_1^i \tilde{N}_2^j \rangle = \langle \tilde{N}_1^i \rangle \langle \tilde{N}_2^j \rangle = 0, \quad (\text{E3})$$

which states that the orientation in two different pixels is not correlated, and the orientations inside each pixel are randomly distributed.

Notice that if one takes the limit $1 \rightarrow 2$ in (E2), it appears that cosmological velocities give a modification in the variance of the velocity field. This is due to the fact that when computing the aberration angle, we kept only the first order term in the velocity. However, we need to make sure that unit vectors have unit norm, as an incorrect normalization brings biases when estimating the variance of $\cos \iota$. Explicitly, for the aberrated direction, one has to consider

$$\tilde{\mathbf{n}} = \frac{\mathbf{n} + \mathbf{v}_\perp}{\sqrt{1 + v_\perp^2}}. \quad (\text{E4})$$

Now we use that the average of a direction vector is such

that $\langle \tilde{N}_i \tilde{N}_j \rangle = (1/3)\delta_{ij}$ hence $\langle (\cos \iota)^2 \rangle = (\mathbf{n} \cdot \mathbf{n})/3 = 1/3$. Then we compute

$$\langle (\cos \tilde{\iota})^2 \rangle = \frac{\langle (\cos \iota)^2 \rangle + \langle (\tilde{\mathbf{N}} \cdot \mathbf{v}_\perp)^2 \rangle}{1 + v_\perp^2} = \frac{\frac{1}{3} + \frac{v_\perp^2}{3}}{1 + v_\perp^2} = \frac{1}{3}. \quad (\text{E5})$$

Hence $\langle (\cos \tilde{\iota})^2 \rangle = \langle (\cos \iota)^2 \rangle$, showing that the variance of the orientation is also not affected by a global velocity flow.

REFERENCES

- Abbott B. P., et al., 2016, *Phys. Rev. Lett.*, 116, 061102
 Abbott B. P., et al., 2019a, *Phys. Rev. X*, 9, 031040
 Abbott B. P., et al., 2019b, *Phys. Rev. D*, 100, 104036
 Abbott R., et al., 2021a, *Phys. Rev. X*, 11, 021053
 Abbott R., et al., 2021b, *Phys. Rev. D*, 103, 122002
 Blanchet L., 2014, *Living Rev. Rel.*, 17, 2
 Bonvin C., Caprini C., Sturani R., Tamanini N., 2017, *Phys. Rev. D*, 95, 044029
 Challinor A., van Leeuwen F., 2002, *Phys. Rev. D*, 65, 103001
 Chen X., 2021, in , *Handbook of Gravitational Wave Astronomy*. p. 39, doi:10.1007/978-981-15-4702-7-39-1
 Dai L., Chluba J., 2014, *Phys. Rev. D*, 89, 123504
 Dalang C., Durrer R., Lacasa F., 2022, arXiv e-prints, p. arXiv:2209.12812
 Domènech G., Mohayaee R., Patil S. P., Sarkar S., 2022, *JCAP*, 10, 019
 Finke A., Foffa S., Iacovelli F., Maggiore M., Mancarella M., 2021, *JCAP*, 2021, 026
 Iacovelli F., Finke A., Foffa S., Maggiore M., Mancarella M., 2022, arXiv e-prints, p. arXiv:2203.09237
 Isoyama S., Sturani R., Nakano H., 2021, in , *Handbook of Gravitational Wave Astronomy*. p. 31, doi:10.1007/978-981-15-4702-7-31-1
 Leyde K., Mastrogiovanni S., Steer D. A., Chassande-Mottin E., Karathanasis C., 2022, arXiv, p. arXiv:2203.11680
 Mancarella M., Genoud-Prachex E., Maggiore M., 2022, *Phys. Rev. D*, 105, 064030
 Mastrogiovanni S., Bonvin C., Cusin G., Foffa S., 2022
 Mukherjee S., Lavaux G., Bouchet F. R., Jasche J., Wandelt B. D., Nissanke S., Leclercq F., Hotokezaka K., 2021, *A&A*, 646, A65
 Sberna L., et al., 2022, *Phys. Rev. D*, 106, 064056
 Sturani R., 2021, in , *Handbook of Gravitational Wave Astronomy*. p. 32, doi:10.1007/978-981-15-4702-7-32-1
 Tamanini N., Klein A., Bonvin C., Barausse E., Caprini C., 2020, *Phys. Rev. D*, 101
 The LIGO Scientific Collaboration et al., 2021a, arXiv, p. arXiv:2108.01045
 The LIGO Scientific Collaboration et al., 2021b, arXiv, p. arXiv:2111.03604
 The LIGO Scientific Collaboration et al., 2021c, arXiv, p. arXiv:2111.03606
 The LIGO Scientific Collaboration et al., 2021d, arXiv, p. arXiv:2112.06861
 Torres-Orjuela A., Chen X., Cao Z., Amaro-Seoane P., Peng P., 2019, *Phys. Rev. D*, 100, 063012
 Torres-Orjuela A., Chen X., Seoane P. A., 2021, *Phys. Rev. D*, 104, 123025
 Toubiana A., et al., 2021, *Phys. Rev. Lett.*, 126, 101105

Vitale S., Biscoveanu S., Talbot C., 2022, arXiv, p. [arXiv:2204.00968](https://arxiv.org/abs/2204.00968)
Yasini S., Pierpaoli E., 2017, *Phys. Rev. D*, 96, 103502
Zhao T., Cao Z., Lin C.-Y., Yo H.-J., 2021, in , Handbook of Gravitational Wave Astronomy. p. 34, doi:[10.1007/978-981-15-4702-7_34-1](https://doi.org/10.1007/978-981-15-4702-7_34-1)